Energy Spectra of Protons from (d,p) Reactions in Heavy Elements*

B. L. COHEN, J. B. MEAD, R. E. PRICE, K. S. QUISENBERRY, AND C. MARTZ
Radiation Laboratory, University of Pittsburgh, Pittsburgh, Pennsylvania

(Received July 27, 1959)

Surveys of proton energy distributions from (d,p) reactions were made on nuclei with $Z>30$ using resolutions of 500 and 80 kev. The gross structure shows broad peaks due to the major nuclear shells, as expected from the fact that (d,p) stripping reactions excite single-particle states; peaks due to the subshell structure can be seen in some cases, especially in the heavier nuclei. The energies of the various peaks do not shift from element to element in the manner expected from simple theory; it is shown that this is not in conflict with neutron cross-section evidence, and possible explanations are proposed. The energy spacing between major shells derived from these measurements allows calculation of the reduced mass for nucleons in nuclei; the result is very different from the predictions of Brueckner theory, but explanations for this discrepancy are advanced. The results and their interpretation given here are in direct conflict with the Wilkinson theory of gamma-ray giant resonances. The energy spectra are very similar at different angles, which indicates that the stripping process is predominant at all angles. Deviations from Butler angular distribution theory at large angles must therefore be due to difficulties in that theory rather than due to the onset of competing process.

INTRODUCTION

IT is well known that (d,p) stripping reactions excite single-particle levels—or excite any given level with a strength proportional to its single particle component.[1] Thus, the cross section for a (d,p) reaction is large when the energy of the neutron it inserts into the nucleus (E_n) is equal to the energy of a single particle level this neutron can occupy. Since the energy of the proton emitted in the reaction (E_p) is rigidly related to E_n by

$$E_p=E_d-E_n-2.2 \text{ Mev} \quad (1)$$

(where E_d is the energy of the incident deuteron), measurements of $\sigma(d,p)$ vs E_p, [the energy spectra of protons from (d,p) reactions], are equivalent to measurements of $\sigma(d,p)$ vs E_n, and are thus suitable for studying the single particle neutron levels. Since single particle levels occur at about the same energy for neighboring elements, strong similarities in the spectra of neighboring elements are expected.

In this paper, we report on a general survey of energy distributions of protons from (d,p) reactions in heavy elements $(Z>30)$. It includes a low resolution survey to determine the gross structure of the single particle level density, and a preliminary high resolution survey. The low resolution survey shows the effects of major shell structures, including the regularities among neighboring nuclei, and some unexpected results on how the positions of the shells shift from element to element. The high resolution survey shows some of the subshell structure, and indicates some of the problems in studying this in detail. The data also has implications for deuteron stripping theory, and gives spacings between adjacent major shells which bears on the question of reduced mass of nucleons in nuclei, and on the Wilkinson theory of gamma-ray giant resonance.

EXPERIMENTAL METHODS AND RESULTS

The low resolution measurements were made by detecting the protons with a CsI(Tl) scintillation crystal, and measuring the resulting pulse-height distributions with a 256-channel pulse-height analyzer. An aluminum absorber was placed in front of the crystal to stop deuterons, tritons, and alpha particles; this necessitated elaborate corrections to the proton energies. States with known (d,p) reaction Q values were used for the energy calibration, and many cross checks of this type were made. The over-all energy resolution in these measurements was about 0.5 Mev except in a few cases where target thickness was the limiting factor. An example of data taken directly from the 256-channel analyzer is shown in Fig. 1.

The types of target and their thicknesses are listed in Table I. Commercial metal foils were used wherever these were available. In other cases, targets were prepared from powdered chemical compounds (usually oxides) by depositing a suspension of these in polystyrene on a one-mil Mylar film. Due to the large

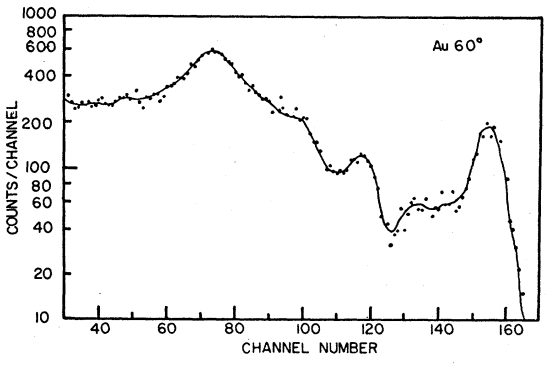

FIG. 1. Energy distribution of protons from (d,p) reactions on Au. This is a typical example of unprocessed data taken with the scintillation detector used in conjunction with a 256-channel pulse-height analyzer. Data of this type was used in constructing the composite low resolution display shown in Figs. 2, 3, and 4.

* Supported by the National Science Foundation and by the joint program of the Office of Naval Research and the U. S. Atomic Energy Commission.

[1] T. Auerbach and J. P. French, Phys. Rev. **98**, 1276 (1955); J. B. French and B. J. Raz, Phys. Rev. **104**, 1411 (1956).

TABLE I. Targets and thicknesses.

A. Foil targets

Element	Thickness (mg/cm²)	Element	Thickness (mg/cm²)
Pb	16.2	Cd	17.1, 11
Au	7.5	Ag	5.0, 10.0
Pt	7	Pd	4.9
W	49.3	Rh	7.0
Ta	14.8	Mo	18.5
Sn	10.7	Nb	12
In	17	Zr	2.3, 7.0
		Zn	2.6

B. Powder targets (on one mil Mylar support)

Element	Material	Thickness (mg/cm²)	Element	Material	Thickness (mg/cm²)
U	$UO_2(NO_3)_2$	2.3	La	La_2O_3	17.7
Bi	Bi metal	4.5	Ba	$BaCO_3$	3.5
Tl	Tl_2O_3	2.9	I	I_2O_5	5.2
Hg	HgO	5.4	Sb	Sb metal	11.3
Er	Er_2O_3	6.1	Ru	Ru metal	2.1
Dy	Dy_2O_3	4.1	Y	Y_2O_3	12.4
Gd	Gd_2O_3	6.3	Sr	SrO	1.4
Sm	Sm_2O_3	10.7	Rb	$RbCO_3$	1.9
Pr	Pr_2O_3	4.3	As	As_2O_3	2.5
Ce	CeO_2	3.5	Te	Te metal	12.9
			Se	Se metal	6.2

C. Special composite targets

Cs	CsI crystal on Mylar support	10 mg/cm²
Ir	Ir-loaded polyethelyne tape	10 and 15 mg/cm², respectively

amounts of carbon and oxygen included, powder targets were used only for measurements at 90° where the energies of protons from (d,p) reactions in light elements are greatly reduced by center-of-mass motion. Nonuniformities and uncertainties in target thickness lead to uncertainties in the energy scale as large as 0.3 Mev in some cases. The data from low resolution surveys taken at 90°, 60°, and 30° are shown in Figs. 2, 3, and 4, respectively.

The high resolution measurements were made by magnetic analysis of the protons with a 60° wedge magnet spectrometer[2] and were detected with photographic plates on the focal plane.[3] The plates were covered with sufficient aluminum absorber to stop deuterons, tritons, and alpha particles. After development, they were scanned with microscopes by counting the number of tracks per unit area as a function of position along the plate. The targets were the same as those used in the low resolution work (see Table I). Except in cases where target thickness was limiting, the energy resolution was about 80 kev. A typical example of the fine structure data is shown in Fig. 5. Some of the results from the fine structure survey are shown in Figs. 6, 7, and 8.

Since the absorber needed to stop the deuterons also stops low-energy protons (or degrades their energy enough to make them indistinguishable from gamma-ray background), these protons could not be studied

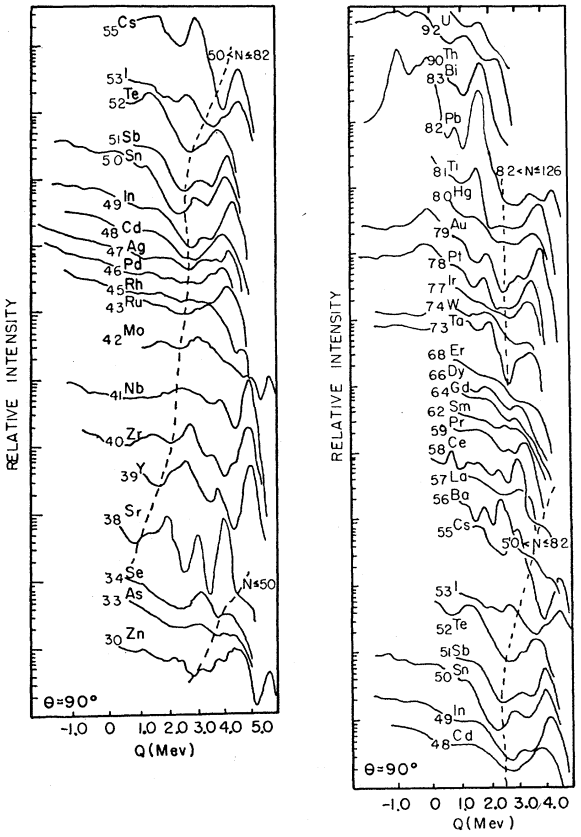

FIG. 2. Low resolution survey of the proton energy spectra from (d,p) reactions on nuclei with $Z>30$. Detection angle is 90°, resolution about 500 kev.

[2] R. S. Bender, E. M. Reilley, A. J. Allen, J. S. Arthur, and H. J. Hausman, Rev. Sci. Instr. 23, 542 (1952).

[3] The authors are greatly indebted to Professor J. R. Cameron who set up the photographic plate detection program.

in the low resolution survey. It was not considered worthwhile to include them in the high resolution survey because of their lack of detailed structure. An intermediate resolution survey of the low-energy portion of the proton energy distributions was therefore made by magnetically analyzing the protons and detecting them with a CsI(Tl) crystal. Since only particles with a given $H\rho$ were incident on the crystal, the protons were easily separated from the other particles and gamma rays by pulse-height analysis ($E_p=2E_d=3E_t$). The spectrum was then measured by determining

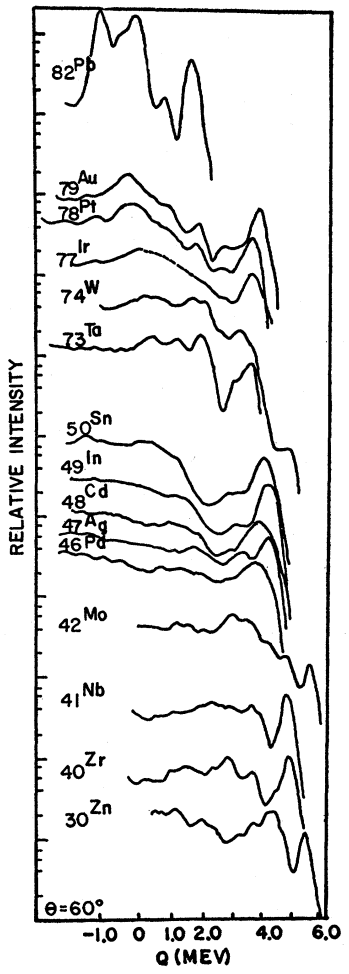

FIG. 3. Low resolution survey of proton energy spectra from (d,p) reactions taken at 60°.

counts per microcoulomb of incident beam for various settings of the magnetic field. All parameters of the system were set to give an over-all resolution of about 200 kev. A typical example of unprocessed data of this type is shown in Fig. 9.

The results of this survey are shown in Fig. 10. Since the time required to measure a spectrum in this manner decreases very rapidly as resolution is reduced (it varies approximately as the fourth power of the resolution), curves such as those in Fig. 10, were obtained in less than one hour each.

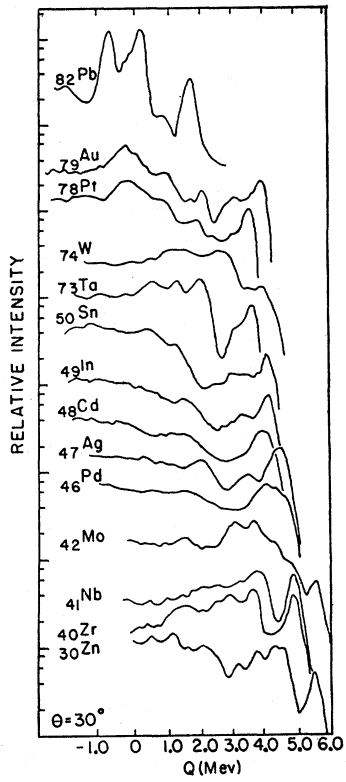

FIG. 4. Low resolution survey of proton energy spectra from (d,p) reactions taken at 30°.

DISCUSSION AND CONCLUSIONS

A. Correlation with Nuclear Shell Structure

It is clear from Figs. 2, 3, and 4 that the energy spectrum is quite independent of angle. Thus, the ensuing discussion will in general refer to the 90° data since it is the most complete.

The gross structure in the region of $Z=42$ to 53 is characterized by a peak at $Q\simeq 4$ Mev followed by a valley at $Q\simeq 2.5$ Mev and a rise to plateau at $Q\simeq 1.5$ Mev. This is the region where the $s_{\frac{1}{2}}$, $d_{\frac{5}{2}}$, $d_{\frac{3}{2}}$, $g_{7/2}$, and

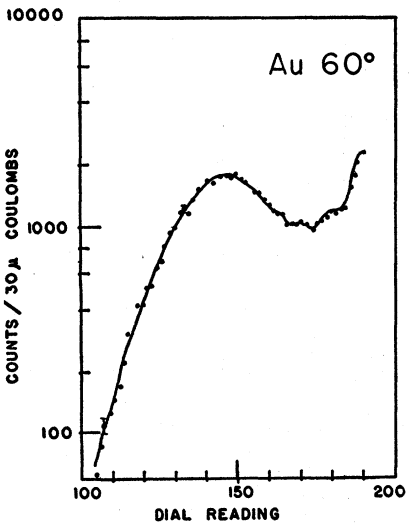

FIG. 5. Low-energy portion of proton spectrum from (d,p) reactions on Au. This is a typical example of data taken with 200-kev resolution using the 60° magnetic spectrometer and scintillation detector. Data of this type was used in constructing Fig. 6.

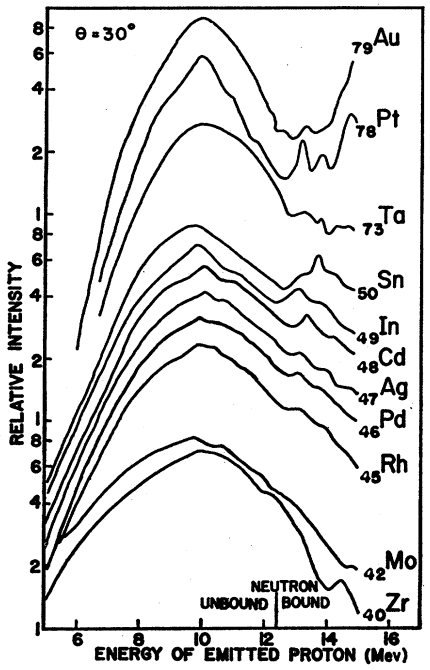

FIG. 6. Intermediate resolution (200-kev) survey of the low-energy portion of the energy spectra of protons from (d,p) reactions.

$h_{11/2}$ levels, comprising the major shell of $50<N\leqslant 82$ (where N is neutron number), are filling; levels corresponding to all of these j values are known to occur in the region of the 4-Mev peak[4] (see for example, Cd^{111} and Sn^{117}). This peak ends abruptly at Ba where the shell is filled. Both of these facts strongly indicate that this peak is due to the filling of single particles levels in the $50<N\leqslant 82$ shell. The fact that single particle levels from a single major shell tend to group together into a relatively narrow band was first pointed out to the author by Lane[5] whose conclusions were based on both theoretical[6,7] and experimental[4] evidence.

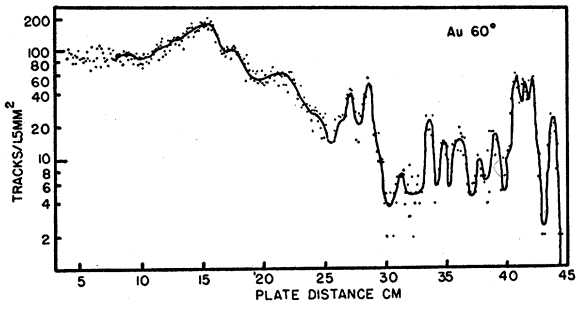

FIG. 7. Fine structure of the energy spectrum of protons from (d,p) reactions on Au taken with the magnetic spectrometer and photographic plates. This figure is representative of data used to compile Figs. 8, 9, 10. Approximate resolution, 80 kev.

[4] D. Strominger, J. M. Hollander, and G. T. Seaborg, Revs. Modern Phys. 30, 585 (1958).
[5] A. M. Lane (private communication).
[6] A. A. Ross, H. Mark, and R. D. Lawson, Phys. Rev. 102, 1613 (1956); 104, 401 (1956).
[7] A. Schröder, Nuovo cimento 7, 461 (1958).

The plateau starting at $Q\simeq 1.5$ Mev would then seem to be due to the filling of single particle levels in the $82<N\leqslant 126$ shell. This interpretation is supported by following this structure from element to element up to the Pt-Au-Pb region; by this time it has moved to $Q\simeq 4$ Mev where it includes many known levels with spins and parities corresponding to $p_{\frac{3}{2}}$, $p_{\frac{1}{2}}$, $f_{\frac{7}{2}}$, $f_{\frac{5}{2}}$, $h_{9/2}$, $i_{13/2}$ which are the single particle levels for $82<N\leqslant 126$. There is further evidence for the surmise that the filling of single particle levels in this shell is responsible for the $Q\simeq 1.5$-Mev plateau in the region $Z=42$–53; this arises from neutron cross-section work[8] which indicates that the p subshell passes through zero neutron energy ($Q=-2.2$ Mev) at $Z\simeq 40$. Since the p subshell is at

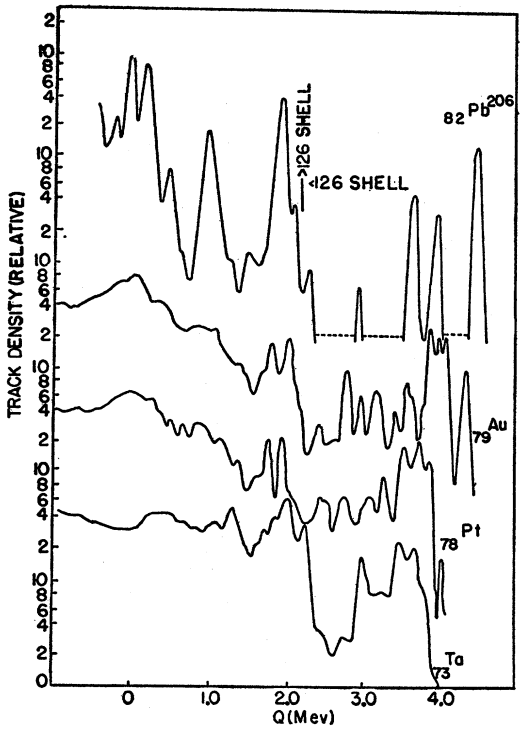

FIG. 8. High resolution (80-kev) proton energy distribution from (d,p) reactions on several heavy elements.

the top of the $82<N\leqslant 126$ major shell,[9] the peak due to the filling of this major shell extends roughly from $Q=1.5$ Mev to $Q=-2$ Mev in this region.

The region $Z=73$ to 83 is characterized by peaks at $Q\simeq 4$ Mev, 1.6 Mev, and 0 Mev. The peak at 1.6 Mev is the highest energy peak for nuclei with $N>126$ (e.g., Pb^{208}, Bi^{209}, etc.) so that the 4-Mev peak must be due to filling levels in the $82<N\leqslant 126$ shell, in agreement with evidence referred to above. The $N>126$ shell then extends roughly from $Q=1.7$ to $Q=-1.0$ Mev in this region. Near the top of this major shell is the s subshell which, according to the neutron data,

[8] H. Feshbach, C. E. Porter, and V. F. Weisskopf, Phys. Rev. 96, 448 (1954).
[9] P. F. A. Klinkenberg, Revs. Modern Phys. 24, 63 (1952).

passes through $Q=-2.2$ Mev at $Z=65$, in good agreement with the above estimate of the extent of the major shell in the region $Z=73$ to 83.

Returning to the lighter element region, we note that for $Z=38$ to 44, there is an extra peak to the right of what we have previously identified as the $Q\simeq 4$-Mev peak in the region immediately above it. In several cases, this extra peak includes known $d_{\frac{5}{2}}$ levels, so that it must be due to the $d_{\frac{5}{2}}$ subshell of the $50<N\leqslant 82$ major shell. This indicates that the $d_{\frac{5}{2}}$ subshell is split away from the rest of the major shell by about 1 Mev. In these nuclei, the remainder of the major shell also seems to be somewhat split up (probably into the $s_{\frac{1}{2}}$ and $d_{\frac{3}{2}}$ subshells; these should be more strongly excited than the $g_{7/2}$ and $h_{11/2}$ subshells) and spread over a wider energy region. The upper extent of this major shell may be estimated from the fact that in accordance with the neutron data, the s-subshell passes through $Q=-2.2$ Mev at $Z=25$; according to the recent work of Schiffer and Lee,[10] it is at about $Q=2$ Mev at $Z=30$.

The splitting of the major shells into subshells is especially well illustrated by the high resolution data in the heavy element region shown in Fig. 8; at least 3 distinct subshells in the $N>126$ major shell can be discerned and traced from element to element from $Z=73$ to 83. This technique is not nearly so successful among the lighter nuclei as evidenced from Figs. 9 and 10. The reason for this may be surmised from the data

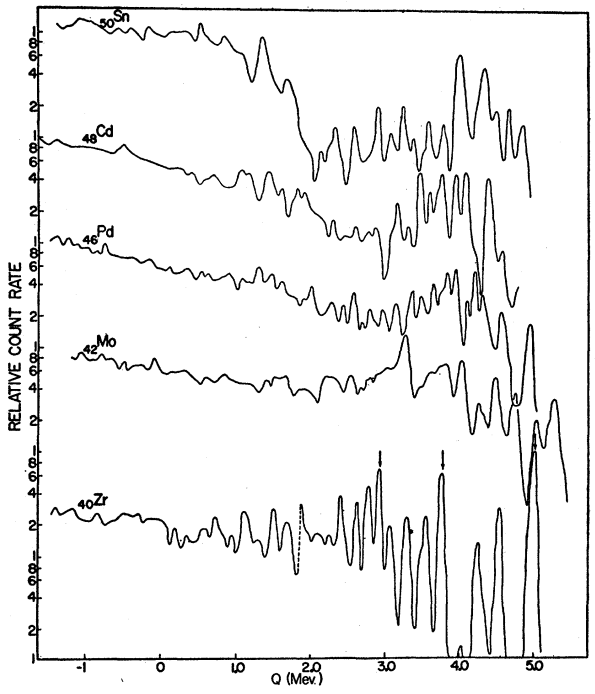

FIG. 9. High resolution proton energy distribution from (d,p) reactions in several intermediate weight elements with even number of protons. The arrows designate known levels in Zirconium. Resolution, 80 kev.

[10] J. P. Schiffer and L. L. Lee, Phys. Rev. **115**, 1705 (1959).

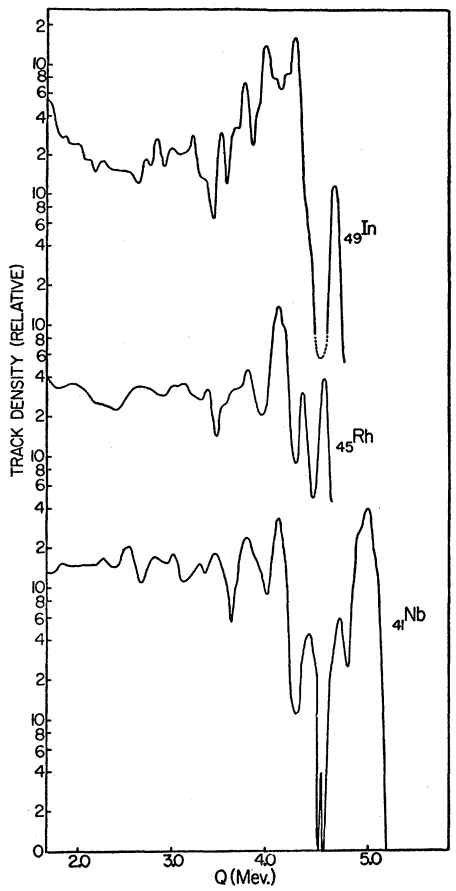

FIG. 10. High resolution proton energy distribution from (d,p) reactions in intermediate weight nuclei with an odd number of protons. Resolution, 80 kev.

for Zr in Fig. 9: the arrows show the states due to the (d,p) reaction on Zr^{90}, and there is evidence that the smaller peaks occurring regularly to the left of these are the corresponding peaks due to other isotopes. It is clear from this that when mixtures of isotopes are bombarded, the subshell structure is washed out, so that the subshell structure in this region can only be studied by use of separated isotopes. An active program of studies using separated isotopes is in progress,[11] but a description of that work is beyond the scope of this paper. The reason for this difference between heavy and medium weight nuclei is not clear, but the evidence for it is unquestionable.

A detailed understanding of the energy spectra from odd proton nuclei, shown in Fig. 10, will be difficult to achieve until more is known about the even proton nuclei, which are much simpler.

Some interest might be attached to nuclei with an odd number of neutrons since these are essentially not represented in Figs. 1 to 6; they exist only as low abundance isotopes of even proton elements. Some data

[11] B. L. Cohen, R. E. Price, and S. Mayo (to be published).

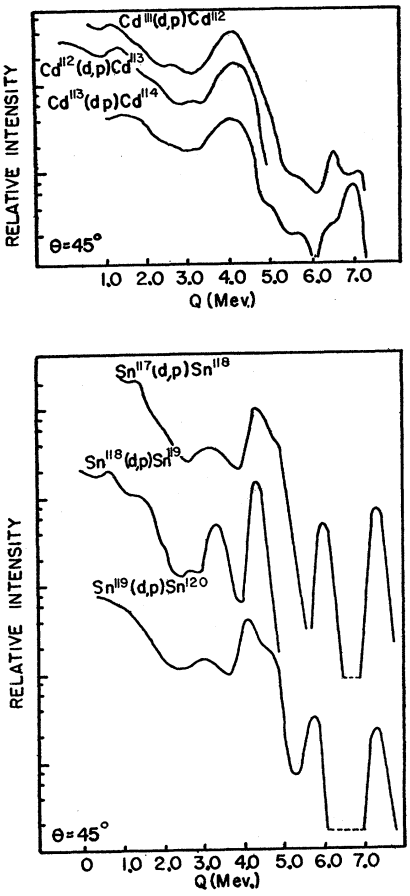

FIG. 11. A comparison of the gross structure of isotopes having an even and odd neutron number. This figure was compiled from photographic plate data for which the resolution was artificially spread to about 500 kev.

on these is shown in Fig. 11 where results for odd neutron isotopes are compared with those for even neutron isotopes of the same elements. The most striking observation from Fig. 11 is that the gross structure peaks occur at the same Q value in even and odd neutron isotopes even though the excitation energy at which they occur differs by more than 3 Mev. This may be explained[5] if one notes that the neutron that is added does not usually form a pair with the odd neutron, so that its binding energy is unaffected by the existence of the odd neutron. The high excitation energy of the resulting nucleus is only high relative to the ground state; that is, to the state that would have been formed if the added neutron had formed a pair. The separation between the $Q\simeq 4$-Mev peak and the ground state is a clear cut determination of the pairing energy, since similar states are involved in each. From Fig. 11, the pairing energy in Cd and Sn is about 3 Mev.

The division between the various shells is shown by the dashed lines in Fig. 2.

B. Shifting of Single Particle Levels with Nuclear Size

Single particle levels occur approximately at energies where the nuclear radius is an integral multiple of half wavelengths. Thus as the mass number increases leading to an increase in nuclear radius, the wavelength for a given level must increase proportionately, causing the energy of the level to drop down lower in the well. If one calculates this effect for a square well with the Feshbach-Porter-Weisskopf parameters,[8] one obtains an energy shift per mass number, $\Delta E/\Delta A$, of

$$\Delta E/\Delta A\simeq 15 \text{ Mev}/A. \quad (2)$$

This corresponds to an energy shift of about 0.4 Mev per atomic number in the region $Z=38$–55, and about 0.2 Mev per atomic number in the region $Z=73$ to 83. It is immediately clear from Fig. 2, that the observed shifts are not nearly that large; an upper limit to their magnitude is about 20% of the value obtained from (2). Similar conclusions are obtained from the structure in the low-energy part of the spectra shown in Fig. 6.

From Fig. 2, it is apparent that most of the energy shifting that does occur is in the immediate neighborhood of closed shells. This is definitely the case in the regions of $N=50$ and $N=82$, but $N=126$ seems to be an exception. When the shell closing at 126 neutrons becomes full, it is no longer excited; the levels from the next shell do not shift, but rather stay fixed, so that there is a sharp discontinuity in the neutron binding energy. However, even including the rapid shifting near closed shells, the over-all shifting is only about half as large as expected from (2).. These results were very puzzling in view of the supposed close agreement between the neutron data of Barschall and others,[12] and the calculations of Feshbach, Porter, and Weisskopf.[8] The latter used a square well, and thus show a shifting in accordance with (2). Since the neutron data is difficult to study in detail with the usual three-dimensional representation, it was replotted from the original data and is shown in Fig. 12.

The positions of the three principle peaks at nonzero energy predicted by the calculations in reference 8 are shown in Fig. 12 by the dashed lines; the attached letters are the angular momentum wave which, being in resonance, causes them. It is clear from Fig. 12 that two of the three predicted peaks are not present at all in the data, whereas the third (which in the theoretical calculations is no more prominent than the others) shifts much less rapidly than the theoretical predictions. The agreement between experiment and theory in the neutron case is much poorer than is generally believed, and there is certainly no evidence in the neutron data contradictory to the lack of shifting found in the present experiments.

In the lack of shifting found in these experiments, there are two phenomena to explain: the fact that the over-all shifting is only about half of the square well

[12] H. H. Barschall, Phys. Rev. 86, 431 (1952); *Neutron Cross Sections*, compiled by D. J. Hughes and J. A. Harvey, Brookhaven National Laboratory Report BNL-325 (Superintendent of Documents, Washington, D. C., 1955).

prediction; and the fact that practically all the shifting occurs over very small mass number intervals, with almost no shifting being observed in two rather extensive mass number intervals. The first may be explained by deviations from a square well in which the top few Mev of the well have a much larger radius than the remainder.[10] Calculations by Baranger and Lee[13] indicate that this explanation is quantitatively satisfactory. The second might be explained by variations of the nuclear radius from the $A^{\frac{1}{3}}$ dependence,[5] or by changes in the depth of the nuclear potential well, V_0; however, any variations of this type would cause irregularities in the angular distributions from elastic scattering, as both effects are sensitive essentially to V_0r^2. Since no such irregularities are observed in elastic proton scattering experiments,[14] these explanations are difficult.

From a broader point of view, positions of energy levels can be affected by variations in any of the terms

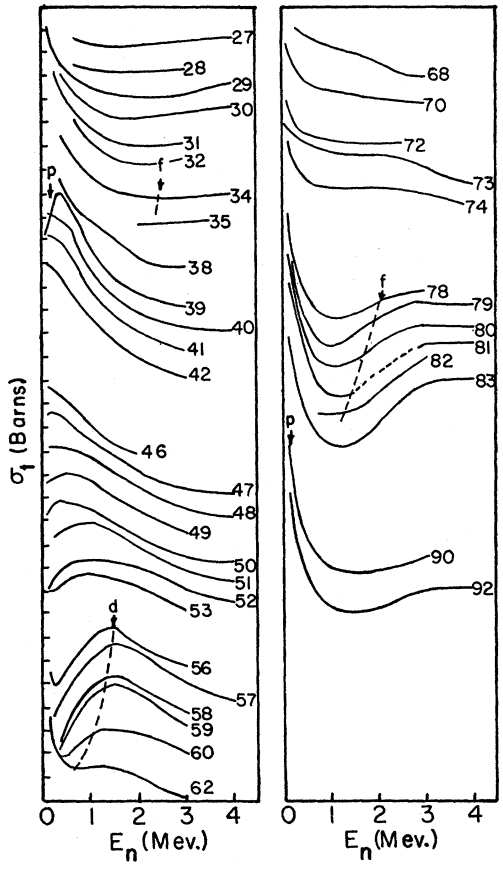

FIG. 12. A replot of the original total neutron cross-section data of Barshall. The dashed lines indicate the positions of peaks in the neutron total cross section as predicted by the optical model.

[13] E. Baranger and C. W. Lee (private communication).
[14] B. L. Cohen and R. V. Neidigh, Phys. Rev. **93**, 282 (1954); B. B. Kinsey, Phys. Rev. **99**, 332 (1955); F. Dayton and G. Schrank, Phys. Rev. **101**, 1358 (1956); N. M. Hintz, Phys. Rev. **106**, 1201 (1957).

TABLE II. Energy changes per added neutron or proton, and total energies for $A=125$ from the Weizacker mass formula.

Number	Type of energy	E/Neutron (Mev)	E/Proton (Mev)	Total energy (Mev)
(1)	Volume	−14	−14	−1750
(2)	Symmetry	6	−6	70
(3)	Coulomb	−0.7	11	300
(4)	Surface	1.8	1.8	300

in the Weizacker mass formula. When a neutron or proton is added to a nucleus of $A\simeq125$, the energy changes and total energies are shown in Table II.

The single particle model being used in this analysis takes into account (1) and perhaps (4); it definitely does not take into account (2) and (3), so that any changes in the sum of these would cause deviations of energy shifts from the single particle model prediction of Eq. (2).

One example of this type would be a surface distortion; if it is assumed to be of the form $1+a_2P_2(\cos\theta)$, the sum of (3) and (4) changes[15] by the fraction $a_2^2/5$. Since this sum is 600 Mev (see Table II), only a very small change in a_2 can cause appreciable deviations from the few tenths Mev shifts per atomic number predicted by the single particle model.

C. Spacings Between Major Shells

In accordance with Fig. 2 and the discussion of Sec. A above, the energy spacing between the centers of consecutive nuclear shells is about 4.5 Mev. This spacing may be used[16] to calculate the reduced mass of nucleons in the nucleus, and the nuclear potential depth. The results for a square well potential with radius $1.45\,A^{\frac{1}{3}}$ are

$$V_0\simeq20 \text{ Mev},$$
$$M^*/M\simeq2.0.$$

This is in sharp disagreement with usual estimates of reduced mass[16,17] which are about $\frac{1}{2}M$. This disagreement would be lessened if the top of the well were assumed to have a much larger radius; but a factor of two increase in nuclear radius would be necessary to eliminate the discrepancy, and this would seem to be quite improbable. Another possible explanation is that the reduced mass is different in excited and normally unoccupied levels than in normally occupied levels.

D. Implications for Wilkinson Theory of Gamma-Ray Giant Resonances

The results reported here and their interpretation in Sec. A are in direct conflict with the Wilkinson theory

[15] N. Bohr and J. Wheeler, Phys. Rev. **56**, 426 (1939).
[16] V. F. Weisskopf, Nuclear Phys. **3**, 423 (1957).
[17] K. Brueckner and C. Levinson, Phys. Rev. **97**, 1344 (1955); L. C. Gomes, J. D. Walecka, and V. F. Weisskopf, Ann. Phys. **3**, 241 (1958).

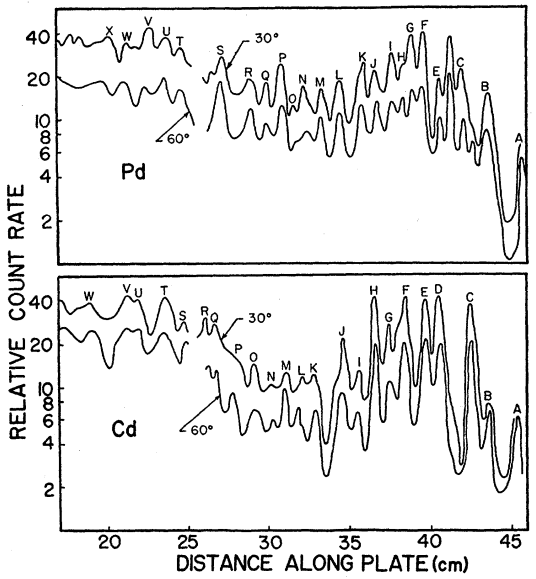

FIG. 13. A comparison between the proton energy spectra from (d,p) reactions on Pd and Cd taken at different scattering angles.

of gamma-ray giant resonances.[18] To illustrate this conflict and present some additional evidence, we will consider in detail two special cases, Zr^{90} and Pb^{208}.

In Zr^{90}, the Wilkinson theory would require a $g_{9/2}$ neutron to be excited to the $h_{11/2}$ level. The energy required to remove a $g_{9/2}$ neutron from Zr^{90} is directly obtainable from the (γ,n) threshold energy; it is about 12.3 Mev. The Wilkinson explanation would then require that an $h_{11/2}$ neutron be *unbound* by about 6 Mev, whereas in accordance with the discussion of Sec. A, it is *bound* by about 4 Mev. (Binding energy $=Q+2.2$ Mev)—a discrepancy of about 10 Mev! The position of the $h_{11/2}$ particle level is known in Pd^{107}, Pd^{109}, Pd^{111}, Cd^{111}, Cd^{113}, Cd^{115}, Sn^{117}, Sn^{119}, Sn^{121}, Sn^{123}, Sn^{125}, and Sn^{127}; in all these cases it is within 0.5 Mev of the ground state which is bound by about 6 Mev. In view of this very slow variation with mass number, it would seem most unlikely that its position would shift by more than a few Mev between masses 107 and 90. In addition, in all cases where the position of the $h_{11/2}$ level is known, it is very close to the $s_{\frac{1}{2}}$ level; the latter is certainly bound by mass 90, since, from the neutron data[8] it passes through zero binding energy at mass 55. One would certainly expect the $h_{11/2}$ level to be more strongly bound than the $3p$ level, but the latter passes through zero binding energy[8] at mass 90. All of these facts strongly support the location of the $h_{11/2}$ level given in Sec. A, as opposed to the Wilkinson theory prediction which is some 10 Mev higher.

Another specific example is Pb^{208}. The Wilkinson theory requires that the giant resonance transition be between the $p_{\frac{1}{2}}$ and $d_{\frac{3}{2}}$ states. A $p_{\frac{1}{2}}$ neutron is bound by 7.4 Mev, so that the $d_{\frac{3}{2}}$ state would have to be *unbound* by about 7 Mev to explain the energy of the giant resonance, whereas from Sec. A, it is *bound* by about 2 Mev—a discrepancy of 9 Mev. Additional evidence that the $d_{\frac{3}{2}}$ level is actually bound by a few Mev comes from its proximity to the $s_{\frac{1}{2}}$ level which goes through zero binding energy[8] at mass 160. From their intensity, the three strong peaks near zero binding in the Pb data of Fig. 8 are expected to be the $s_{\frac{1}{2}}$, $d_{\frac{5}{2}}$, and $d_{\frac{3}{2}}$ particle states.

The choice of two closed shell examples in no way implies that the discrepancy between Wilkinson theory and the discussion of Sec. A is limited to those cases. All the effects mentioned vary slowly from nucleus to nucleus, with no very large discontinuities at closed shells.

E. Implications for Reaction Theory

It is almost universal in deuteron stripping studies to find that angular distributions do not fall off at large angles nearly as rapidly as predicted by theory; this indeed is the case in the present experiment. The usual explanation for this is that the protons emitted at large angles do not result from stripping.

In the present experiments, the energy distributions are the same at various angles as evidenced by Figs. 2, 3, and 4, and by the similarity in fine structure at various angles as shown by Fig. 13. Further evidence for this may be seen in the angular distribution measurements of Gove.[19]

However, all the characteristics of the energy distribution are explained by the fact that these reactions do proceed by deuteron stripping. One must therefore conclude that the difficulty at large angles is with stripping angular distribution theory rather than with the onset of competing processes.

The shape of the low-energy portion of the proton energy distributions shown in Fig. 6 are very puzzling since the position of the peak is virtually independent of atomic number. It is believed that this part of the spectrum is due to deuteron break-up, but this matter is being further studied both experimentally and theoretically.

ACKNOWLEDGMENTS

The authors are greatly indebted to Dr. J. R. Cameron who set up the photographic plate detection system, to the cyclotron operation crew and the microscope scanning group for their very essential services, and to Dr. A. J. Allen for support and encouragement. A very special debt of gratitude is due to Dr. A. M. Lane for several important suggestions.

[18] D. H. Wilkinson, Physica 23, 1039 (1956).

[19] H. E. Gove, Phys. Rev. 81, 364 (1951).